A theoretical investigation of the fracture energy of heterogeneous brittle materials

1994 J. Phys.: Condens. Matter 6 1857

(http://iopscience.iop.org/0953-8984/6/10/005)

J. Phys.: Condens. Matter 6 (1994) 1857–1868. Printed in the UK

A theoretical investigation of the fracture energy of heterogeneous brittle materials

T Chelidze†, T Reuschlé‡ and Y Guéguen§

† Institute of Geophysics, Georgian Academy of Sciences, Tbilisi, Georgia
‡ EOPGS, CNRS URA 1358, 5 rue René Descartes, 67084 Strasbourg Cédex, France
§ Géosciences Rennes, Bâtiment 15, Campus Beaulieu, Avenue Gal Leclerc, 35042 Rennes Cédex, France

Received 29 June 1993, in final form 20 December 1993

Abstract. It is shown that the fracture surface energy of heterogeneous brittle materials (polycrystals, composites, ceramics, rocks) depends on their microstructural characteristics, namely the fractal properties of the network of microcracks. A quantitative approach for calculation of fracture energy from microcrack network fractal parameters is suggested. Very high experimental values of fracture energy for heterogeneous brittle materials can be easily explained in the framework of the fractal model.

1. Introduction: the fractal nature of fracture

It is well known from experiments that the fracture energy G of a composite material is much larger than that of homogeneous ones. We restrain ourselves to brittle heterogeneous materials where processes such as plastic deformation are negligible. For example the fracture surface energy of quartz crystals is of the order of 1 J m^{-2} while the fracture energy of quartz sandstones reaches hundreds of J m^{-2} (table 1) [1]. This has even led some experts to conclude that the concept of fracture energy is invalid for heterogeneous materials. Here we define a heterogeneous material as a system that is not necessarily chemically or mineralogically heterogeneous: heterogeneity may appear in form of grain boundaries, pores or cracks.

Let us consider a sample containing a population of cracks. As for a single crack, the total mechanical energy of the system (sample + loading apparatus) varies by an amount of δE_m (<0) when the crack population evolves (by propagation of existing cracks or nucleation of new cracks). At the same time, the creation of new crack surfaces costs an amount of energy proportion to the created surface δA. We define the proportionality coefficient as twice the fracture surface energy γ_c. On the other hand we define G, the crack extension force, as the ratio of the mechanical energy released during the creation of new crack surfaces over the created surface area. For a single crack the criterion of evolution is that the propagation of the crack is possible if G is at least equal to G_c, the critical crack extension force, defined by

$$G = G_c = -\delta E_m/\delta A = 2\gamma_c \tag{1}$$

which simply means that the mechanical energy decrease has to be greater or equal to the energy consumed by the surface creation. For a population of cracks, this criterion

0953-8984/94/101857+12$19.50

Table 1. After [1].

Crystals	Fracture surface energy γ_c (J m^{-2})
Quartz, synthetic	
$(10\bar{1}1)$	0.41
$(\bar{1}011)$	0.5
$(10\bar{1}0)$	1.03
Quartz, fused	3.7
Calcite	
$(10\bar{1}1)$	0.27–0.35
Rocks	
Quartz rocks	
Fontainebleau sandstone	7-27
Berea sandstone	10
Val d'Illiez sandstone	49
Alpnach sandstone	47
Calcite rocks	
Carrara marble	35
Solnhofen limestone	12
Ekeberg marble	20–50
Red Öland limestone	19
Danby marble	40–50
Holston limestone	12

can be generalized by looking at all possible evolutions of this population. The criterion of fracture will then be that at least one possible evolution leads to a mechanical energy decrease greater than or equal to the energy consumed by surface creation. Obviously we have neglected energy losses due to friction on crack surfaces, acoustic emission, heating and other non-varnishing entropy variations. By doing so the criterion of propagation takes the same form as (1). In this case γ_c may be seen as a macroscopic quantity that makes the link between the new surfaces created and the energy it costs to create them, if we were able to measure this energy. By neglecting energy wells other than the surface creation, we underestimate the G value necessary to propagate cracks. This means that in the following model our derived γ_c values should be lower than the observed ones. Indeed this is what happens as we will see later. We will now use G for fracture surface energy, omitting the factor of two.

From (1), we infer that the growth of crack surfaces decreases the mechanical energy of the system. In the following we omit the subscript c and assume that $G = G_c$. The great discrepancy between G of composites and that of crystals can be explained quantitatively as a result of a classical approach [2], ignoring real complicated fracture structures present in heterogeneous deformed media (figure 1(a)). Experiments show that the real structure of fracture is quite different, and that the total surface of microcracks is very large (figure 1(b)) and hence a lot of energy should be spent to create it. This fact is not usually taken into account because unless a special technique is applied for visualization of the microcrack network [3], which is mainly concentrated in the so-called process zone [4] (figure 1(b)), one observes only one trace of this network, namely the macrocrack, which divides the sample into two parts. Accordingly the whole energy that has been spent on the formation of a large number of microcracks is ascribed to a sole rupture with the surface area much smaller than the overall surface of microcracks. As a result the apparent fracture energy G_a is much larger than the true fracture energy G_0. The question is: what formalism can provide a quantitative basis for evaluation of G_0, which has an apparent value G_a?

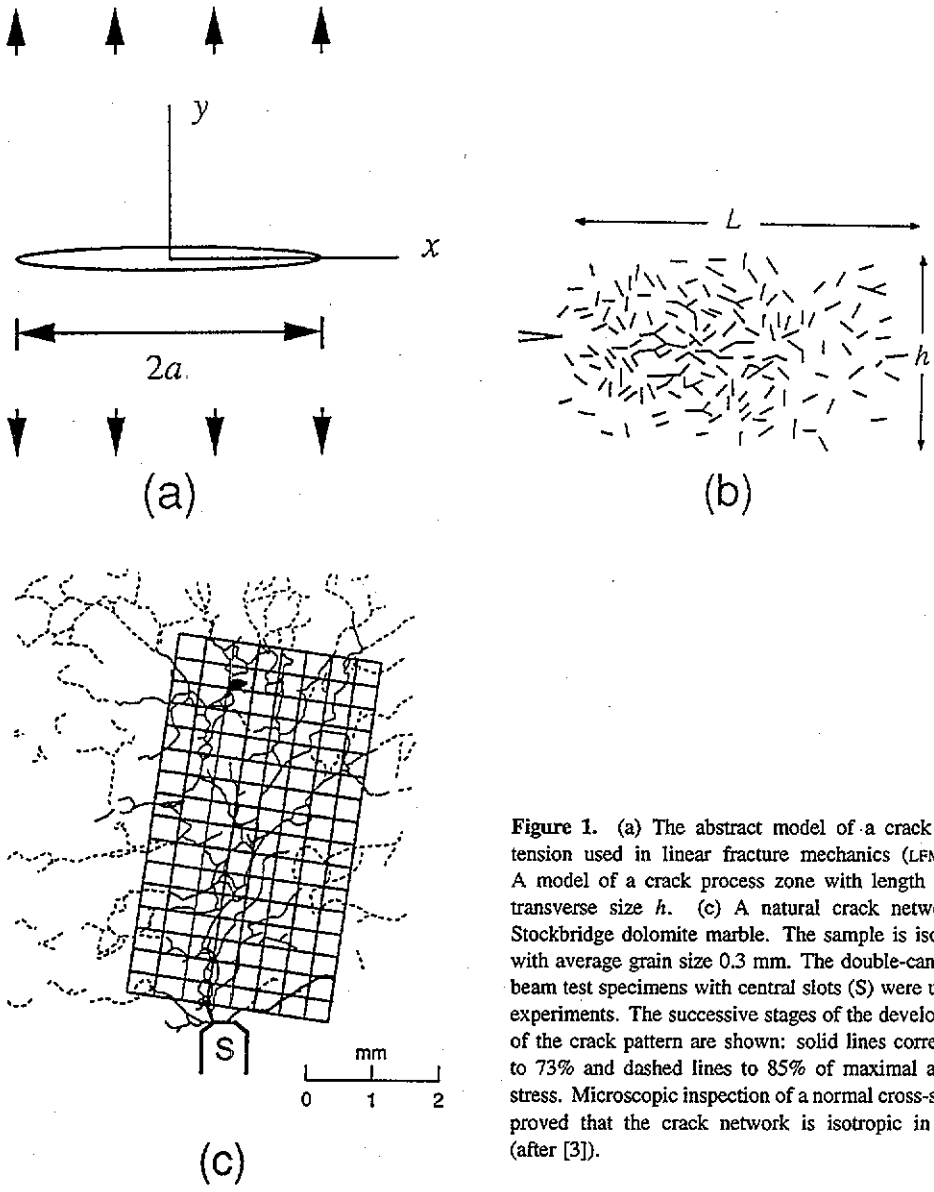

Figure 1. (a) The abstract model of a crack under tension used in linear fracture mechanics (LFM). (b) A model of a crack process zone with length L and transverse size h. (c) A natural crack network in Stockbridge dolomite marble. The sample is isotropic with average grain size 0.3 mm. The double-cantilever beam test specimens with central slots (S) were used in experiments. The successive stages of the development of the crack pattern are shown: solid lines correspond to 73% and dashed lines to 85% of maximal applied stress. Microscopic inspection of a normal cross-section proved that the crack network is isotropic in space (after [3]).

As a rule experiments on fracture energy measurements are realized in such a way that essential microstructural parameters are not available. In order to obtain these parameters, a detailed microscopical study of the process zone is needed, and this is more the exception than the rule. Nevertheless the paper of Nolen-Hoeksema and Gordon [3] reveals microstructural details that are necessary. Figure 2 shows that the fracture of a relatively homogeneous polycrystal (dolomite marble) with a thin groove under traction does not follow a single plane as is predicted by linear fracture mechanics (LFM). Instead a three-dimensional microcrack network is formed near the tip of the groove. Furthermore it is evident from figure 2 that the microcrack network does not initiate at the groove tip as follows from LFM but quite far from it. That means that even at loads approaching 60–80% of breaking load local differences between stress and strength dominate over global stresses.

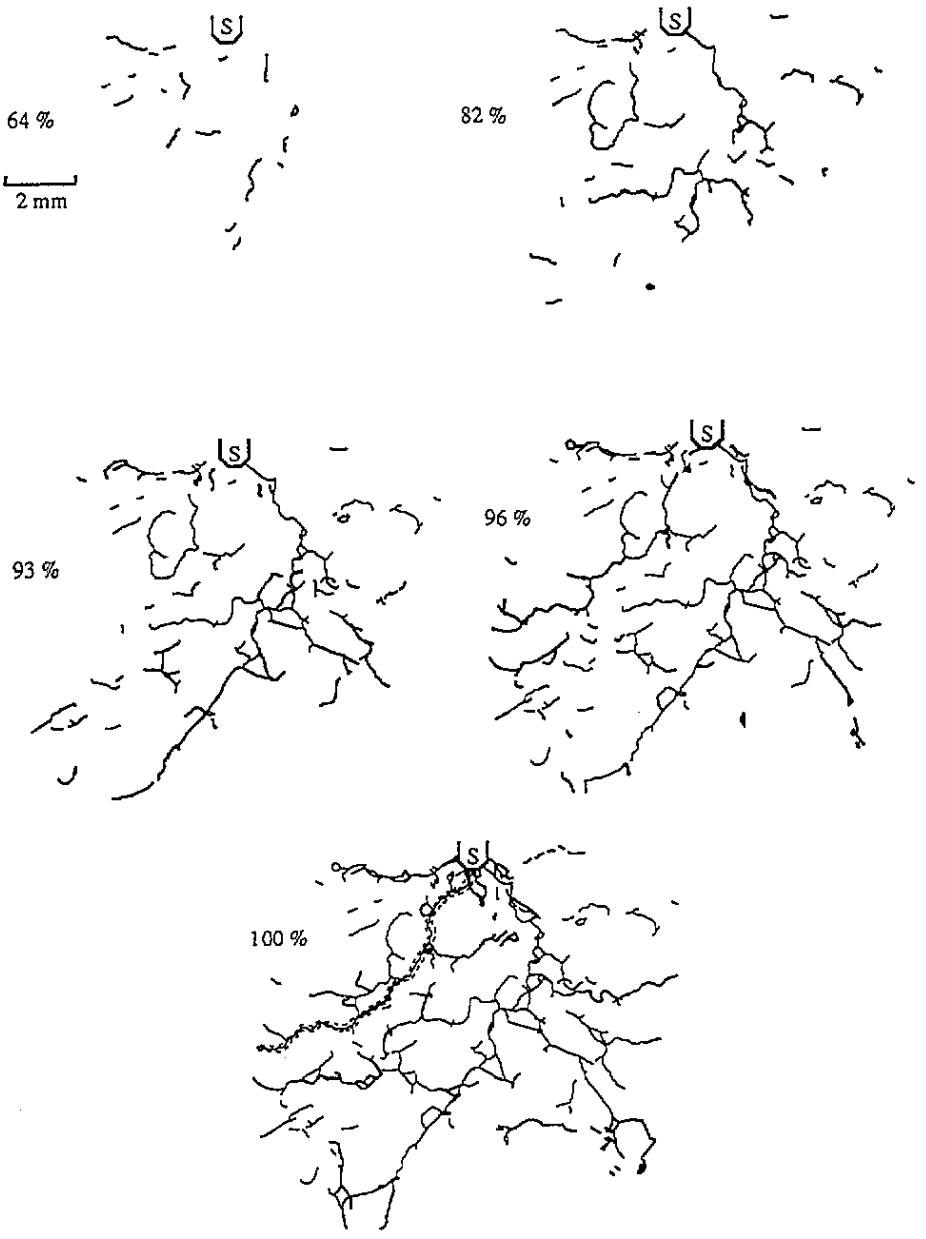

Figure 2. Successive stages of development of a microcrack network near the tip of a slot (S); percentages of maximal stress are indicated. New portions of microcracks are shown in bold lines. In the last panel the main rupture trace is shown by dashed lines (after [3]).

So, in contradiction to the widely developed growth models of fracture, namely diffusion-limited aggregation (DLA) [5], the crack network does not grow from some definite point (seed) but it is rather stacked from separate elementary ruptures and their clusters. Thus the process looks more like percolation or cluster–cluster aggregation process than DLA [6]. The first examination of the structures shown in figures 1(c) and 2 leads us to

suggest that it is fractal.

2. Fractal dimension and fracture energy

Now if the object is fractal, it should be self-similar and the number of elementary cells in squares with successively increasing sizes should scale, according to [4]. An iteration process can then be conducted, starting with an initial elementary cell. This initial elementary cell in our case is a large square $L_0 \times L_0$. At a second stage the elementary cell is defined as a square $L_0/2 \times L_0/2$ and so on, except for the last iteration, where the scale was reduced 50 times. At each iteration the number M of elementary cells that intercept a fracture is counted. Such cells are labelled 'destroyed cells'. The results are given in table 2. The fractal dimension D_2 of a network of cracks for given cross-section of specimen is

$$D_2 = \log M_i / \log L_i \tag{2}$$

where M_i and L_i are respectively the number of destroyed cells and size of the system in units used at the ith iteration. Figure 1(c) shows only stages 1–4 of the iterative process in order to not blur the picture. The results, given in table 2, indicate a fractal dimension $D_2 = 1.6$, which is that of the planar cross-section of the object [8]. The bulk fracture structure should have fractal dimension $D_3 = D_2 + 1$, because stacking of thin layers of (isotropic) fractals with $D_2 = 1.6$ results in a structure with $D = D_3 = 2.6$.

Table 2.

Stage of iteration (i)	1	2	3	4	5	6
Total number of elementary cells in the object	1	4	16	64	256	2500
Size L of elementary cell in units of the initial one	1	$\frac{1}{2}$	$\frac{1}{4}$	$\frac{1}{8}$	$\frac{1}{16}$	$\frac{1}{50}$
Linear size of object in reduced units—quantity L_i in (2)	1	2	4	8	16	50
Number M_i of destroyed cells	1	3	11	27	75	441
Ratio of number of destroyed cells to total number of cells	1	0.75	0.69	0.42	0.292	0.176
Fractal dimension $D_2 = \log M_i / \log L_i$	1	1.58	1.73	1.58	1.56	1.56

There are many experimental studies proving the fractal dimension of fragmentation to be 2.5. Such results are obtained for broken coal, chimney rubble after a nuclear explosion, basalt after the impact of a projectile, synthetic and natural fault gouges [9] and systems of tectonic faults [10], so this figure seems to be universal for delocalized isotropic fracture. Note that the value of $D = 2.5$–2.6 is close to the 3D infinite percolation cluster dimension $D = 2.5$, though theoretical models give different thresholds for percolation and elasticity and therefore different fractal dimensions for these two critical structures.

Thus it seems reasonable to use a fractal approach for evaluation of the 'mass' M of ramified crack networks. The definition of M depends on the mode of evolution of the heterogeneous structure, namely, whether it is fractal or homogeneous, which in turn depends on the ratio of the characteristic size L' of the system and the correlation length L'_c. In the following we assume that L and L_c are dimensionless lengths expressed in units of the size of an elementary object of the heterogeneous system, that is, the sample grain size l:

$$L = L'/l \qquad L_c = L'_c/l. \tag{3}$$

Depending on the ratio of the system size, that is of the length of the fractured (process) zone L to the correlation length of the fractal microcrack network L_c, two limiting cases should be distinguished:

(i) $L < L_c$, the system is in the fractal regime;
(ii) $L > L_c$, the system is in the homogeneous regime.

By definition G is a product of the specific fracture energy g_0 and the total surface area A_0 of the crack network, which naturally should be proportional to the mass M of the network of cracks:

$$A_0 \propto M \tag{4}$$

where M is dimensionless.

When $L < L_c$ (fractal regime), the total mass of cracks including the main rupture is

$$M \propto L^D \tag{5}$$

according to the mass definition in the fractal regime [7] and hence

$$G \propto g_0 L^D. \tag{6}$$

The apparent specific fracture energy g_a is usually obtained by dividing the total measured fracture energy G by the apparent surface area A_a, which is Euclidian and thus can be expressed in terms of the crack size (or process zone length) as a quantity proportional to L^{d_c}. Here d_c is the Euclidian dimension of a planar or linear crack. Let us assume that $d_c = 2$. Then

$$g_a \propto G/L^{d_c} \tag{7}$$

or using (6)

$$g_a \propto g_0 L^{D-d_c}. \tag{8}$$

This means that in the fractal regime g_a is larger than the true value g_0 as D is larger than d_c ($D = 2.6$; $d_c = 2$) and increases with lengthening of the microcracked area or process zone L (figure 1(b)). If $D = d_c$ the apparent energy g_a is equal to the true energy g_0.

When $L > L_c$ (homogeneous regime), the process zone contains so many supergrains with size L_c that it can be considered to be homogeneous. In this case the mass of the object of size L is the product of the mass L_c^D of supergrains and the number of such supergrains in the considered volume, which is $(L/L_c)^d$. In our case L^d is the volume V of the process zone and L_c^d is the volume of the Euclidian figure (cube) that covers the supergrains. Thus from [7] we obtain

$$M = L_c^{D-d} V = L_c^{D-d} L^d \tag{9}$$

where for bulk processes $d = 3$.

Then the total amount of energy due to the creation of crack surfaces distributed in the volume V of the process zone is

$$G = g_0 L_c^{D-d} V \tag{10}$$

where $V = whL$, and w, h and L are accordingly width, height and length of the process zone. The apparent specific fracture energy g_a is equal to G divided by the apparent crack surface area wL:

$$g_a = G/wL = L_c^{D-d} h g_0. \tag{11}$$

For an isotropic network of cracks $w = h = r$ where r is the transverse size of the process zone. This parameter can be expressed in units of correlation length L_c:

$$r = nL_c \tag{12}$$

where n is the number of supergrains of size L_c over the distance r. Then from (11) and (12)

$$g_a = n g_0 L_c^{(D+1)-d} \tag{13}$$

or

$$g_0 = g_a / n L_c^{(D+1)-d}. \tag{14}$$

The apparent specific fracture energy in the homogeneous regime does not depend on the process zone length L, as in the fractal regime (8). However, it depends on the fractal dimension D of the microcrack network and process zone transverse size n, expressed in units of L_c. The larger n and D, the larger is the ratio g_a/g_0: because usually $L_c = L_c'/l > 1$ and $(D + 1 - d) > 0$, or in other words, the larger the 'thickness' of process zone and the finer the microcrack network in this zone, the larger the deviation of apparent specific fracture energy from the true one. Thus from (14) it follows that in order to calculate the true fracture energy g_0 of a heterogeneous material in the homogeneous regime it is necessary to know besides the apparent fracture energy G_a such parameters as the correlation length L_c of the network of cracks, the process zone effective radius n in units of L_c and the fractal dimension D of the crack network.

If G_a is measured in the fractal regime it depends on sample size and in order to evaluate g_0 we need to know L and D. If the fractal dimension of the crack network in the process zone does not change with its growth the true fracture energy can be obtained as the slope of the G versus $\log L$ curve. It is evident from table 2 that the fracture structure is fractal up to lengths $L_f = 0.5L_0$, i.e. on the scale less than the process zone characteristic transverse size $L_p = nL_c$. For boxes with side $L = L_p$ the dimension of the process zone is not fractal: $D = d = 2$, and for these scales the structure is homogeneous. This means that expression (14) should be used for calculation of fracture energy. Note that even in the homogeneous regime the fractal dimension enters the formula for G as the mass M of the object is defined in terms of correlation length L_c, which is now a new natural representative volume size or size of supergrain.

In order to evaluate g_a/g_0 for experimental data (figure 1(c)) it is necessary to extract n and L_c values from them. It is known that L_c is approximately equal to the size of the largest void in the fractal network. According to figure 1(c) the size of the largest void is 2 mm or $L_c = 7$ in units of grain size l, which is 0.3 mm. The same figure gives for the characteristic transverse size of the process zone a value of 8 mm or in units of L_c, $n = 4$. Then from (14) it follows that

$$g_a/g_0 = 4.7^{0.6} \simeq 13$$

i.e. in this particular case the apparent specific fracture energy is more than ten times larger than the true one. From table 1 it follows that g_a for calcite rocks varies between 12 and 100 J m^{-2} while g_0 for the calcite crystal is 0.6 J m^{-2}. Thus the ratio g_a/g_0 varies between 30 and 170. In our calculations we take as the natural elementary unit size the grain size l. If instead of l we consider as elementary the grain facet size l_f the value of L_c should be roughly tripled because $l_f = l/3$ (figure 1 in [3] reveals nearly hexagonal grains of calcite by electron microscopy). Then the ratio g_a/g_0 approaches 40, which is a little nearer to the experimental value, 130 J m^{-2}, given in [3] for this sample, and fits in the fracture energy set of data for calcite rocks ($g_a/g_0 \simeq 40$) quoted in table 1. It should also be taken into consideration that energy can be lost by friction on crack faces, acoustic emission and heating. In addition the pattern of cracks used in this analysis corresponds to 85% of maximal stress. This is why our figures should be considered as a lower limit for the g_a/g_0 ratio. The important point is that it is possible nevertheless to infer an approximate value of this ratio by the measurement of few geometrical parameters of the crack network. The general conclusion is that if the correlation length is of the order of 10 elementary units (grain or facet size) and the process zone also contains approximately 10 correlation lengths in the transverse direction then the results shown in table 1 are easily interpreted in terms of fractal energy of fracture.

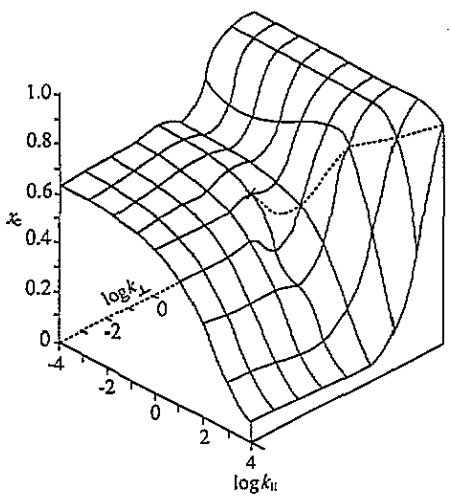

Figure 3. The surface of the percolation threshold in (x_c, $\log k_\parallel$, $\log k_\perp$)-space for a 32 × 32 square lattice (after [11]).

3. Transition from Euclidian to fractal fracture

In nature both fractal and Euclidian modes of fracture can be observed. Understanding of the transition from the Euclidian to the fractal pattern in fracture structures can be gained by considering the model of anisotropically correlated percolation. Major points of this model are (i) elementary ruptures interact due to overlapping of their (scalar) stress fields, giving rise to correlation effects and (ii) at the same time the action of global deviatoric stresses or anisotropy inherent to the material leads to the existence of preferred directions

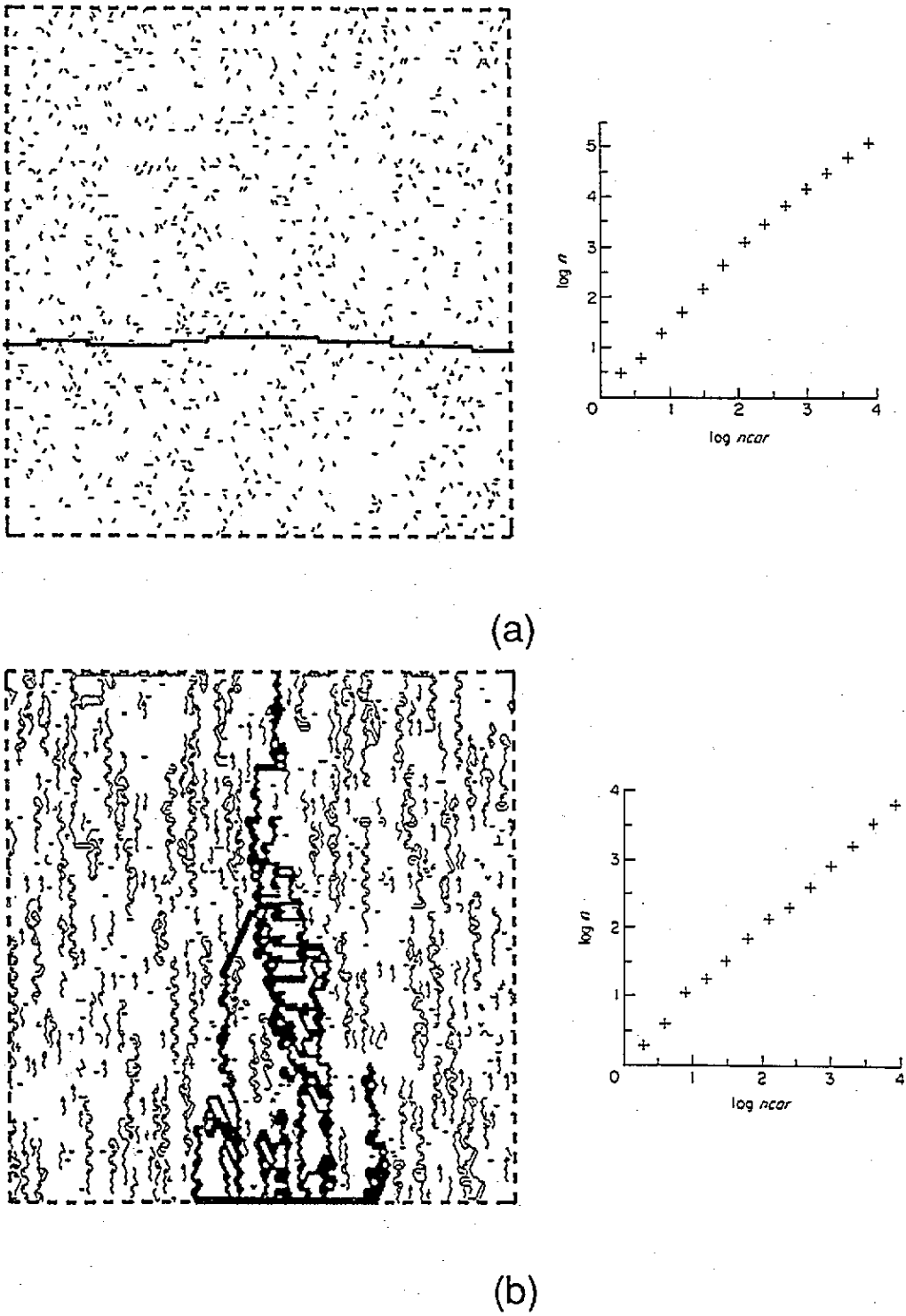

Figure 4. Macroscopic fracture (bold lines) and its fractal dimension in a 128 × 128 triangular lattice for (a) vertical traction and (b) uniaxial vertical compression (after [12]).

in the arrangement of elementary ruptures. Thus both correlation and anisotropy should be taken into account simultaneously. In [11] this process has been simulated on the square lattice of nodes. To introduce anisotropic correlation two different correlation parameters $k_\perp$ and $k_\parallel$ are used for two perpendicular directions. These correlation parameters show how many times the probability of a site being occupied when having an occupied neighbour in the horizontal direction ($k_\parallel$) or the vertical direction ($k_\perp$) on a square lattice is higher or lower than the probability of being occupied randomly. By assuming that an occupied site is equivalent to an elementary crack, this kind of model is an illustration of how to take into account correlation and anisotropy effects in the propagation of cracks. The results of simulation for a 32×32 square lattice are represented in figure 3, which shows how the site percolation threshold x_c depends on anisotropic correlation factors $k_\perp$ and $k_\parallel$. It is obvious that variations of x_c are quite significant. The cross marks the point that corresponds to the random case, i.e. $k_\perp = k_\parallel = 1$. Here we need to damage 60% of the nodes in order to obtain the infinite cluster. The left part of the diagram with negative $\log k_\perp$ and $\log k_\parallel$ (repulsive interaction) is relatively stable with x_c approximately the same as for the random case. For large values of $\log(k_\parallel/k_\perp)$, i.e. extremely strong anisotropic correlation (lower right side of the diagram) x_c is quite small: actually a line of damaged sites is enough to create an infinite cluster. This area should correspond to the LFM domain and is realized at very high ratio of correlation factors, namely when $k_\parallel/k_\perp$ approaches 10^4. Very large positive correlations (upper part of the plot) lead to the necessity of 'crushing the lattice into dust' to obtain an infinite cluster and so $x_c = 1$. Despite the fact that these results were obtained on finite lattices, the value of 0.6 for x_c in the random case shows that the obtained percolation threshold values are not too far from theoretical values (0.593 for random site percolation on a square lattice). This means that the surface character is reliable and will be preserved by increasing the lattice size, though some details may vary. The percolation threshold surface shown in figure 3 can be considered as a characteristic of the number of microcracks that are necessary to create the macroscopic rupture and hence some characteristic of the fracture energy for different fracture patterns. This model is an illustration of how combining correlation effects (stress concentrations due to the presence of cracks) by increasing $k_\perp$ or $k_\parallel$ and anisotropy by changing the ratio $k_\parallel/k_\perp$ leads to the transition from Euclidian ($x_c \to 0$) to fractal fracture ($x_c > 0$).

It is interesting to note that the transition from Euclidian to fractal fracture has been observed in computer simulations of failure of a triangular lattice of bonds depending on the mode of loading [12]. For traction and shear the main rupture is almost linear with $D = 1.05$ (figure 4(a)). Under uniaxial or biaxial compression the fracture pattern is much more ramified and leads to D-values of about 1.4–1.5 (figure 4(b)). These varying patterns reflect competition between local interactions and the global stress field.

The supposed model can also explain the well known grain size dependence of fracture energy of polycrystals [13], showing a maximum in energy consumption on the meso-grain scale (B) and low values of G for both large (C) and fine (A) grains (figure 5). The fine-grained material is almost as homogeneous as glass or crystal. We can therefore assume that both the correlation length and process zone are of the order of the grain size l. Then $L'_c/l = L_c = 1$ and $n = 1$ (in other words $D = d$). As a result g_a is close to g_0. At the coarse-grain end of the diagram the correlation length is so large that it exceeds the sample size. Thus effectively the material again is homogeneous, but this is a finite-size effect and it should disappear in larger samples. From our conjecture it follows that the correlation length of the crack network can be obtained from these data as the sample size for which G drops steeply. Thus maximal energy consumption should be observed at

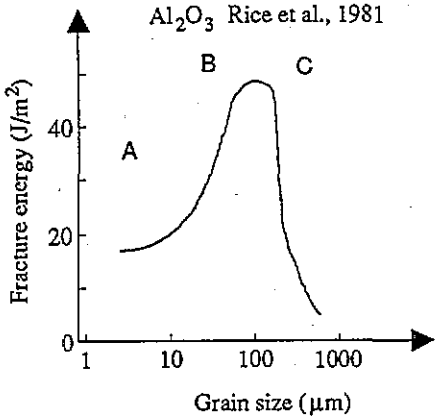

Figure 5. Fracture energy versus grain size for alumina samples (Al_2O_3) (after [13]).

maximal ramification of the microcrack network in the process zone when L_c and/or n are large.

Another phenomenon that can be explained in the framework of the fractal fracture energy concept is crack arrest in a heterogeneous material after dynamic propagation during which rupture is almost linear (or planar). Decrease of local stress near the tip of a running crack at the final stage of crack propagation makes other local stresses near inhomogeneities more and more important. As a result the crack begins to ramify, creating a fractal structure with large energy consumption, and this eventually leads to crack arrest.

4. Conclusion

We have shown that the fracture surface energy of heterogeneous brittle materials depends on the fractal properties of the network of microcracks. We have proposed a theoretical approach to derive a fracture energy value from microcrack network fractal parameters. When applied to experimental data, this model of fractal fracture may explain the observed high fracture energies for aggregates when compared to single-crystal values.

It seems promising to develop further the fractal fracture energy concept by taking into account additional features of percolation structures such as ramification, lacunarity and anisotropic correlation and also try to solve some inverse problems, namely to define the fractality of fracture pattern from the known ratio g_a/g_0 and L_c, to define anisotropic correlation factors from fractograms and so on. Practical applications of the fractal approach can be envisioned, such as designing durable composites by the control of L_c and n in the process zone.

References

[1] Atkinson B K and Meredith P G 1987 *Fracture Mechanics of Rock* ed B K Atkinson (London: Academic) p 477
[2] Liebowitz H (ed) 1968 *Fracture: An Advanced Treatise* vols 1–7 (New York: Academic)
[3] Nolen-Hoeksema R G and Gordon R B 1987 *Int. J. Rock Mech. Min. Sci.* **24** 135
[4] Swanson P L 1987 *J. Geophys. Res.* **92** 8015

[5] Meakin P, Li G, Sander L M, Yan H, Guinea F, Pla O and Louis E 1990 *Disorder and Fracture* ed J C Charmet, S Roux and E Guyon (New York: Plenum) p 119
[6] Chelidze T 1982 *Phys. Earth Plan. Int.* **28** 93
[7] Aharony A 1986 *Fragmentation, Form and Flow in Fractured Media, Annals of Israel Physics Society 8* (Bristol: Hilger) p 79
[8] Chelidze T and Guéguen Y 1987 *Int. J. Rock. Mech. Min. Sci.* **24** 135
[9] Turcotte D L 1992 *Terra Nova* **4** 4
[10] Chelidze T and Gugunava N 1990 *Dok. Acad. Nauk. SSSR* **312** 1095 (in Russian)
[11] Kolesnikov Yu M and Chelidze T 1985 *J. Phys. A: Math. Gen.* **18** 273
[12] Reuschlé T 1992 *Terra Nova* **4** 591
[13] Rice R W, Freiman S W and Becher P F 1981 *J. Am. Ceram. Soc.* **64** 345